

# Microwave Characterization of Nanostructured Material by Modified Nicolson-Ross-Weir Method

J. Y. Wang<sup>1</sup>, J. Tao<sup>1\*</sup>, L. Severac<sup>2</sup>, D. Mesguich<sup>2</sup>, Ch. Laurent<sup>2</sup>

<sup>1</sup>LAPLACE, Toulouse Université, CNRS, INPT, UPS, INP-ENSEEIH, 2 rue Camichel, F-31071 Toulouse cedex 7, France

<sup>2</sup>CIRIMAT, Toulouse Université, CNRS, INPT, UPS, Université Paul-Sabatier, 118 route de Narbonne, F-31062 Toulouse cedex 9, France

\* E-mail: [tao@laplace.univ-tlse.fr](mailto:tao@laplace.univ-tlse.fr)

## Introduction

Nanostructured materials and nanocomposites have specific properties thanks to their nanoscale and are serious candidates in mechanical, electrical, chemical and environmental applications. Among their many physical properties, their capacity to interact with electromagnetic waves is particularly interesting as a potential source of new functionalities<sup>1-3</sup>.

In this paper, the simultaneous characterization of the permittivity and the permeability of the samples of a new nanostructured material will be presented in the frequency band 40 MHz and 1600 MHz. First, the Nicolson-Ross-Weir algorithm (NRW)<sup>4,5</sup> will be applied to the scattering parameters measured with a vector network analyzer on a microstrip transmission line cell on which a rectangular slab sample is added. The effective complex permittivity and permeability of central part consisting of the plate on a reference planar line will be deduced. This central part will then be modeled as a section of multilayer planar transmission line including the sample to be characterized. The permittivity and permeability of the materials will be determined by an inverse modeling method based on the use of the full-wave modified transverse resonance method (MTRM)<sup>6</sup>.

The weak point of the NRW algorithm lies in the fact that the reactive electromagnetic energy in the discontinuities regions is not taken into account. This reactive energy contributes to modifying the effective length of the central section, thus introducing a potentially large source of error. We propose an iterative procedure to minimize the error induced by the presence of this

reactive energy by modeling it by a lumped reactive element, deduced from a 3D electromagnetic simulation of a simple junction. This technique has been validated on several samples of known dielectric materials, and will be applied to a sample of nanostructured materials.

## Material

Random composite materials combining a ferromagnetic metal within an oxide matrix have demonstrated their potential as double negative materials (DNM)<sup>1-3</sup>. DNM exhibit both negative electric permittivity and negative magnetic permeability leading to unique properties in terms of wave propagation with high breakthrough potential, especially in fields such as optics (superlenses) or electromagnetic cloaking (invisibility cloaking)<sup>7</sup>. Such composites are bulk 3D materials with isotropic electromagnetic properties originating from their composition and microstructure.

An Fe-Al<sub>2</sub>O<sub>3</sub> composite powder was prepared by a method involving the selective reduction of an oxide solid solution. First, the mixed oxalate (NH<sub>4</sub>)<sub>3</sub>Al<sub>0.8</sub>Fe<sub>0.2</sub>(C<sub>2</sub>O<sub>4</sub>)<sub>3</sub>.nH<sub>2</sub>O is obtained by precipitation in alcohol. Heat-treatment in air (at 400°C for 2 hours) leads to the decomposition of the oxalate and the formation of the amorphous (Al<sub>0.8</sub>Fe<sub>0.2</sub>)<sub>2</sub>O<sub>3</sub> solid solution<sup>8</sup>. Heat-treatment in H<sub>2</sub> (1100°C, 5 hours) then produces the reduction of the ferric ions to metallic iron, forming the Fe-Al<sub>2</sub>O<sub>3</sub> composite powder<sup>9</sup>.

The iron content in the composite is equal to 12.0 vol.%, well below percolation threshold evaluated at about 30 vol.%. The specimen is thus an insulating material. The so-obtained powder

was consolidated by spark plasma sintering (SPS) (1400 °C, 3 min, 50 MPa) in order to obtain pellets 8 mm and 50 mm in diameter and 1.5 mm thick (PNF2-Toulouse, Dr. Sinter 2080, SPS Syntex Inc., Japan). Then, the 50 mm pellet was cut into rectangle 28.5 x 21.5 mm for the electromagnetic measurements. A typical FEG-SEM image (recorded in backscattered electron chemical composition mode to enhance contrast) of a cross-section of the Fe-Al<sub>2</sub>O<sub>3</sub> composite reveals that the Fe particles (appearing as white dots on the image) are homogeneously dispersed into the Al<sub>2</sub>O<sub>3</sub> matrix (Fig. 1). The diameter of the Fe particles was measured on hundreds of particles on such images and the distribution (inset in Fig 1) lies in the range 0.2 μm to 5.7 μm in diameter, with a median value of 0.7 μm.

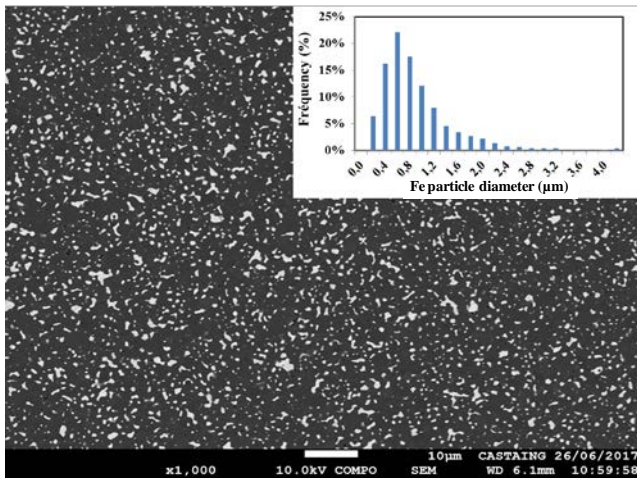


**Figure 1:** FEG-SEM image of a cross-section of the 12 vol.% Fe-Al<sub>2</sub>O<sub>3</sub> composite and the corresponding Fe particle diameter distribution.

**Description of measurement cell**

In this paper, we have opted for the multilayer microstrip line structure in which the sample under test (SUT) is placed on the top of a reference microstrip line (Fig. 2). The SUT loaded section is inserted between two know reference microstrip lines. Both characteristic impedance and propagation constant are different from those of reference microstrip line due to the different permittivity and permeability of the SUT. Reflection occurs at two extremities of SUT. A

delay also exists compared to the microstrip line without SUT. The scattering parameters will be measured by using a vector network analyzer between two SMA connectors (Fig. 2(b)). The use of thru-reflect-line (TRL) calibration procedure leads to the determination of S parameters between the two ends of SUT loaded section.

If each part of measurement cell can be considered as fully loaded transmission lines, Nicholson-Ross-Weir (NRW) algorithm permits the deduction of wide frequency range permittivity and permeability of SUT<sup>4,5</sup>. This measurement method is a non-resonant one, and as others non resonant methods the broadband measurement will be effectuated but the measurement results will be less accurate compared to resonant methods, particularly with regard to dielectric and magnetic losses.

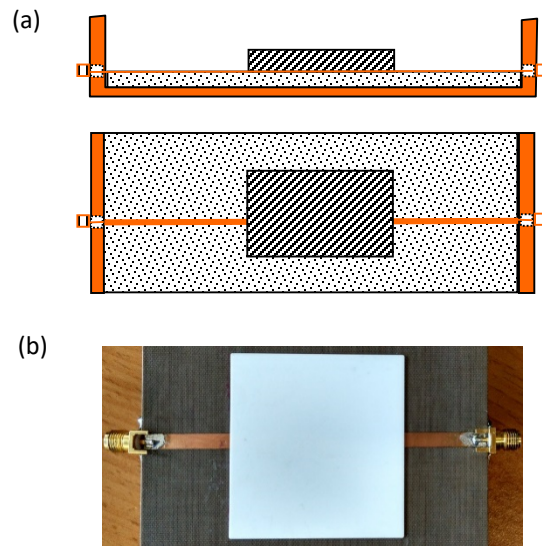


**Figure 2:** The quasi-TEM measurement setup in (a) a schematic view, and (b) an image of the real structure with an alumina plate.

**Extraction method of material properties**

Once the S parameters obtained by the vector network analyzer in the microstrip cell loaded with a thin rectangular SUT, the determination of the complex permittivity and permeability of the material pass through an inverse modeling procedure. This procedure includes a comparison

of the measurement results and numerical simulation with trial values of the relative complex permittivity and permeability. An optimization algorithm is used then to adjust the trial values in order to minimize the deviation between the simulated and measured  $S$  parameters.

Generally speaking, the numerical simulation involves a 3D electromagnetic simulation software, such as commercial HFSS or CST, or other electro-magnetic modeling methods developed by university researchers, such as the multimodal variational method (MVM)<sup>10</sup>. The 3D simulations require significant computer resources in RAM and computing time. Here we propose an alternative solution with the modified version of Nicolson-Ross-Weir (NRW) algorithm, which combines the original method and a 2D electro-magnetic formulation for the determination of the fundamental characteristics of an equivalent transmission line.

**A. NRW algorithm for fully filled transmission line structure**

In the case of homogeneous transmission lines with the middle section fully filled with a different material of length  $d$ , taking the two ends of the central section as reference planes, the parameters  $S$  are given by<sup>11</sup>

$$S_{11} = \frac{(1-P^2)\Gamma}{1-P^2\Gamma^2}, \quad S_{21} = \frac{(1-P^2)P}{1-P^2\Gamma^2},$$

where  $P = e^{-\gamma d}$  is the propagation exponent of the TEM mode in the fully filled central section, and  $\Gamma = (Z - Z_0)/(Z + Z_0)$  is the reflection coefficient, where  $Z$  and  $Z_0$  correspond respectively to the characteristic impedance of the central section and the reference line. The direct inversion of this system of equations leads to the following relationships,

$$\Gamma = X + s_1 \sqrt{X^2 - 1}, \quad s_1 = \pm 1,$$

$$P = \frac{V_1 - \Gamma}{1 - V_1 \Gamma} = |P| e^{j \arg(P)},$$

where  $V_1 = S_{11} + S_{21}$  and  $X = (1 - S_{21}^2 + S_{11}^2)/(2S_{11})$ .

In most of the cases, the reference TEM line has very low losses, hence  $\epsilon_1 \cong \epsilon_0 \epsilon_{r1}$  and  $\mu_1 \cong \mu_0$ . By noting the central line as fully filled with material to be measured,

$$\epsilon_2 = \epsilon_0 (\epsilon_{r2}' - j \epsilon_{r2}'' ) = \epsilon_0 \epsilon_{r2} (1 - j \tan \delta_\epsilon),$$

$$\mu_2 = \mu_0 (\mu_{r2}' - j \mu_{r2}'' ) = \mu_0 \mu_{r2} (1 - j \tan \delta_\mu)$$

the unknown relative permittivity and permeability will be given by

$$\sqrt{\frac{\mu_{r2} \epsilon_{r1}}{\epsilon_{r2}}} = \frac{1 + \Gamma}{1 - \Gamma},$$

$$\sqrt{\epsilon_{r2} \mu_{r2}} = \frac{-j \cdot \arg(P) - \ln|P|}{k_0 d}$$

where  $k_0 = 2\pi f \sqrt{\mu_0 \epsilon_0}$  is the propagation constant in free space.

**B. Application of the NRW formulation for multilayer planar structures**

The explicit relations between the propagation constant, the characteristic impedance of a TEM mode of fully-filled transmission line, and the parameters of the constituent material, no longer exist in the cases of multilayer planar structures. If for the conventional lines, such as simple microstrips or coplanar lines, the approximate explicit formulations exist, for the others, a numerical simulation tool is necessary, especially for the multilayer structures<sup>6</sup>. A series of design curves will be obtained in a given frequency range, corresponding respectively to the effective relative permittivity and permeability, and the characteristic impedance, with each curve obtained with a trial value for sample's permittivity and permeability. These curves constituent a data base for the interpolation purpose during the inverse modeling procedure.

An example is shown here with a square alumina plate of a 50.8-mm length and a 0.5-mm thickness. The characteristic of the substrate of reference microstrip line are shown in Table 1. In our measurement system, the other parameters of the reference microstrip line are the substrate thickness,  $h = 1.524$  mm, and the central conductor

width and thickness,  $w = 4.257\text{mm}$  and  $t = 35\mu\text{m}$ , respectively. The cell has been designed to operate between 200 MHz and 1.6 GHz, when the relative permittivity of the material does not exceed 15. The use of MTRM<sup>6</sup> on this structure with trial relative permittivity varying between 9 and 12 lead to the effective relative permittivity as shown in Fig. 3(a). Once the measurements carried out by a vector network analyzer, the effective relative permittivity of the central section were obtained by application of the NRW algorithm. The results are given in Fig. 3(b). Finally, the extracted relative permittivity is shown in Fig. 3(c).

**Table 1.** Frequency dependent parameters of an AD255C substrate

Property	1 MHz	10 GHz
Relative permittivity	2.55	2.55
Loss tangent	0.0011	0.0014

**C. Modification of the NRW formulation with discontinuity effect correction**

The determination of the reflection coefficients in the preceding formulation depends only on the relative characteristic impedances between the reference microstrip line and the partial loading by the alumina sample. This is true in the absence of the higher order modes on either side of the junction of the two lines. This is the case for homogeneous TEM lines. However, the planar case with introduction of the sample above the central stripline naturally leads to the presence of evanescent modes. This will introduce reactive energy accumulation in the vicinity of the discontinuities planes. In accordance with the nature of reactive energy, the length of the central section seen by fundamental mode will be different from the actual length. Instead of the actual value  $d$ , it is necessary to introduce  $d_{eff}$  as a function of the frequency.

For each frequency, after the simulation by one of the numerical methods<sup>10</sup>, the equivalent length will be deduced as a function of the geometry and the relative permittivity value proposed for the material to be measured. The evolution of the corrected length  $dl_1$  as a function

of frequency, and of the estimated relative permittivity in the case of alumina sample, were simulated. The new estimated values of the sample were compared to those derived directly from the NRW formulations. These new values better correspond to those expected in the range between 9 and 11 as expected (Fig. 4).

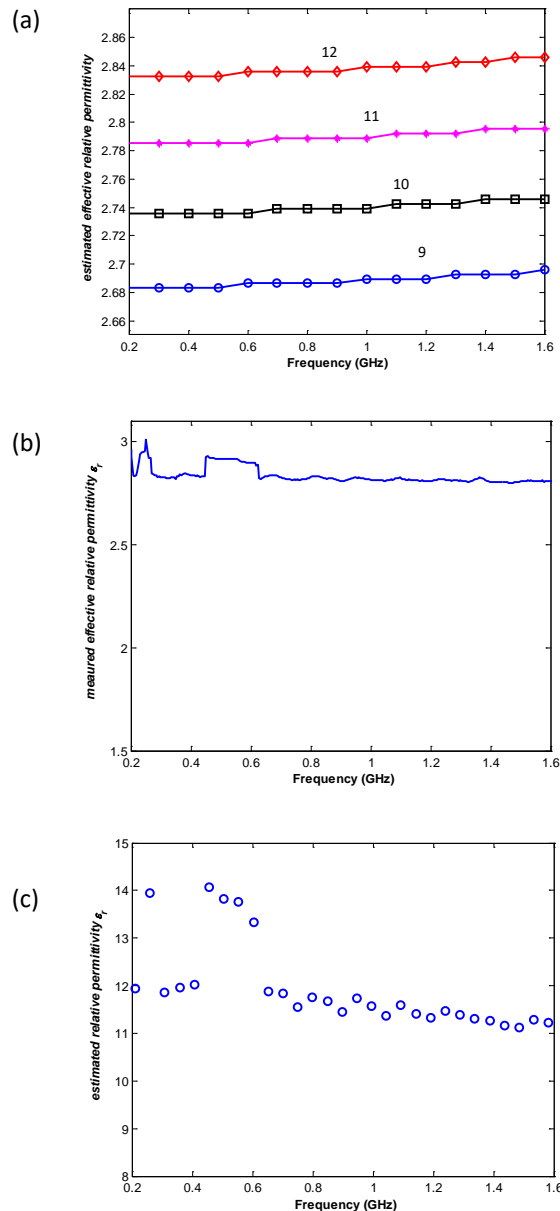


**Figure 3:** Characteristics of multilayered microstrip line: (a) Estimated effective relative permittivity by TRM, with trial relative permittivity varying between 9 to 12. (b) Measured effective permittivity. (c) Extracted sample's relative permittivity.

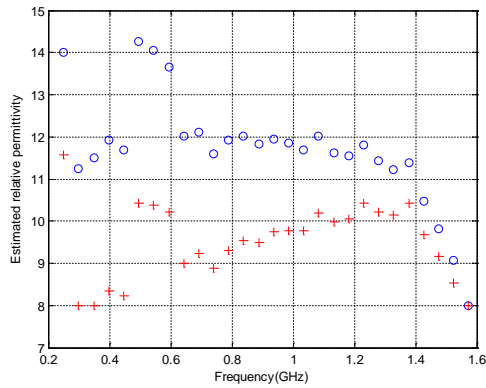


**Figure 4:** Comparison between new (+) and old (o) estimation values.

**Application for nanostructured sample**

Several Fe-Al<sub>2</sub>O<sub>3</sub> composite samples were prepared. Figure 5 shows a rectangular plate cut from the 50 mm pellet and two 8 mm pellets. All were metallized on one side. The rectangular plate was the subject of our research here, in order to extract its complex permittivity and complex permeability. The Fe-Al<sub>2</sub>O<sub>3</sub> composite plate dimensions are 1.47-1.50 mm thickness, 28.51 mm width, and 21.54 mm length.

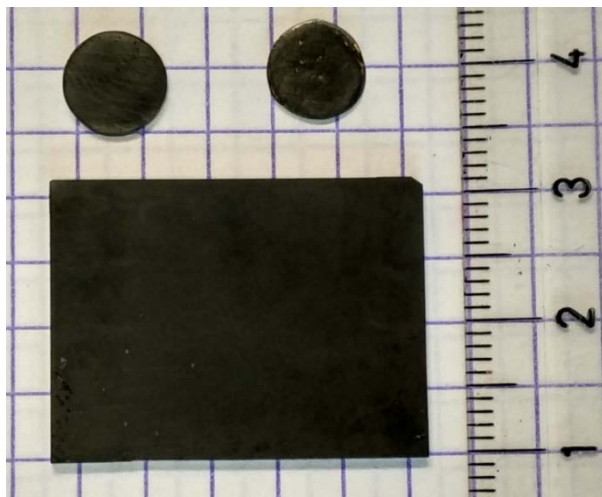


**Figure 5:** Fe-Al<sub>2</sub>O<sub>3</sub> composite prepared by spark plasma sintering (SPS).

After applying the NRW algorithm to the measurement performed with the rectangular Fe-Al<sub>2</sub>O<sub>3</sub> composite, the raw results of the complex effective permittivity and permeability are shown, respectively, in Figs. 6 and 7.

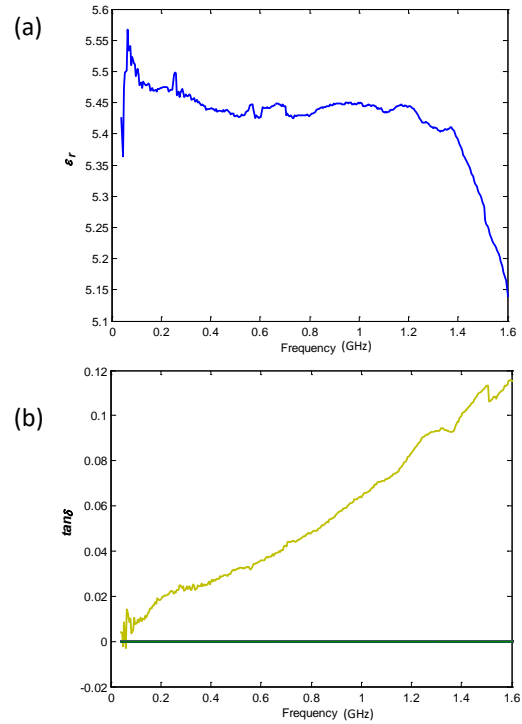


**Figure 6:** Real (a) and imaginary (b) parts of the effective relative permittivity.

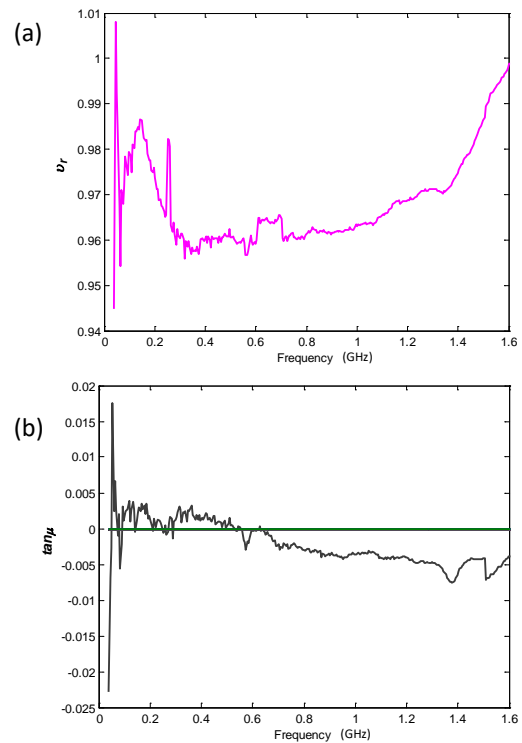


**Figure 7:** Real (a) and imaginary (b) parts of the effective relative permeability.

By using the inverse modeling method proposed in the previous section, we have deduced the estimated values of the complex permittivity, as well as its complex permeability, both given in Figs. 8 and 9. The SUT shows significant losses and exhibits magnetic properties.

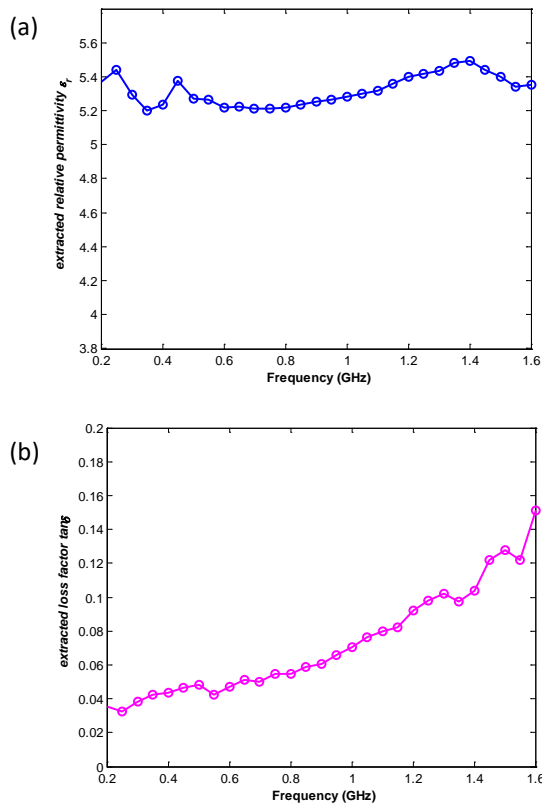


**Figure 8:** Real part (a) and loss factor (b) of the relative permittivity extracted by the inverse modeling method.

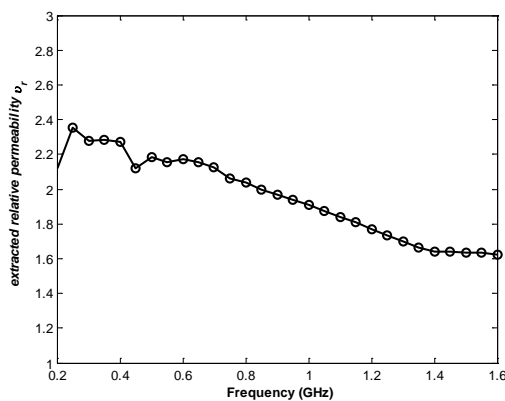


**Figure 9:** Relative permeability extracted by the inverse modeling method.

### Conclusions

A modification of the Nicholson-Ross-Weir formulation has been proposed for the simultaneous extraction of the permittivity and the permeability of a material in a multilayer planar transmission line configuration. The new formulation was successfully tested on a thin plate-like alumina sample. The application of the technique to a Fe-Al<sub>2</sub>O<sub>3</sub> composite material allowed the determination of the electrical and magnetic properties of this material. Significant losses have been observed due to the magnetic nature of the sample.

### For further reading

1. Zhang, Z., R. Fan, et al., *J. Mater. Chem.*, 2013, **1**, 79-85
2. Shi, Z., R. Fan, et al., *J. Mater. Chem.*, 2013, **1**, 1633-1637
3. Shi, Z., R. Fan, et al., *Adv. Mater.*, 2012, **24**, 2349-2352
4. Nicolson, A.M., G. F. Ross, *IEEE Trans. on IM*, 1970, **19**, 377-382.
5. Weir, W. B., *Proc. IEEE*, 1974, **62**, 33-36.
6. Tao, J., *IEEE Trans. MTT*, 1992, **40**, 1966-1969.
7. Pendry, J.B., D. Schurig, et al., *Science*, 2006, **312**, 1780-1782
8. Devaux, X., Ch. Laurent, et al., *Nanostruct. Mater.*, 1993, **2**, 339-346
9. Laurent, Ch., A. Rousset, et al., *J. Mater. Chem.*, 1993, **3**, 513-518
10. Tao, J., et al., *23<sup>th</sup> EuMC*, 1993, 662-664.
11. Rothwell, E. J., et al, *PIER*, 2016, **157**, 31-47.

### About the Authors



**Jingyi Wang** is currently a PhD student in LAPLACE-ENSEEIH-T-INP, Toulouse, France. She received her B.Sc. and M.Sc. degrees (in 2010 and 2013, respectively) in test and measurement technology and Instrumentation from School of Mechano-electronic Engineering, Xidian University, Xi'an, China. Since 2014, Ms. Wang has been working on computational electromagnetics, supported by the China Scholarship Council. Her main research is about modelling and applications of numerical methods in electromagnetics, including 2D and 3D analyses of the coaxial and micro-strip measurement cells.

E-mail: [jywang@laplace.univ-tlse.fr](mailto:jywang@laplace.univ-tlse.fr)



**Junwu Tao** was born in Hubei, China, in 1962. He received his B.Sc. degree in electronics from the Radio Engineering Department, Huazhong (Central China) University of Science and Technology, Wuhan, China, in 1982; the Ph.D degree (with honors) from the Institut National polytechnique of Toulouse, France, in 1988, and the Habilitation degree from the University of Savoie, France, in 1999. From 1983 to 1991, Dr. Tao was with the electronics laboratory of ENSEEIHT, Toulouse, France, where he worked on the application of various numerical methods to 2- and 3-D problems in electromagnetics, and on the design of microwave and millimeter-wave devices. From 1991 to 2001 he was with the microwave laboratory (LAHC) at the university of Savoie, Chambéry, France, where he was an associate professor in electrical engineering and involved in the full-wave characterization of discontinuity in various planar waveguides, and in nonlinear transmission line design. Since September 2001 he is a full professor at the Institut National Polytechnique of Toulouse, where he is involved in the numerical methods for electromagnetics, microwave and RF components design, microwave and millimeter-wave measurements, and microwave power applications.

E-mail: [tao@laplace.univ-tlse.fr](mailto:tao@laplace.univ-tlse.fr)



**Laura Severac** is a PhD student in Materials Sciences at Toulouse University (Université Paul-Sabatier), currently working at the Interuniversity Center for Materials Research and Engineering (CIRIMAT), in the Nanocomposites and Carbon Nanotubes team. She got her MSc in Materials Sciences at Toulouse University. Her research focuses on the preparation of ceramic-matrix composites using spark plasma sintering.

E-mail : [severac@chimie.ups-tlse.fr](mailto:severac@chimie.ups-tlse.fr)



**David Mesguich** is Assistant Professor in Materials Chemistry at Toulouse University (Université Paul Sabatier). He is part of the Nanocomposites and Carbon Nanotubes team working at the Interuniversity Center for Materials Research and Engineering (CIRIMAT) where he works on nanopowders including nanocarbon synthesis by Catalytic Chemical Vapor Deposition and preparation of ceramic- and metal-matrix nanocomposites and carbides, both as powders and bulk materials sintered by SPS.

E-mail: [mesguich@chimie.ups-tlse.fr](mailto:mesguich@chimie.ups-tlse.fr)



**Christophe Laurent** is a Full Professor of Materials Chemistry at Toulouse University (Université Paul-Sabatier). He is currently serving as Director of CIRIMAT, the Interuniversity Center for Materials Research and Engineering, where he formerly headed the Nanocomposites and Carbon Nanotubes team (1998-2015). He got his BSc and MSc degrees in Chemistry, and his Doctor in Materials Sciences degree (PhD) at Toulouse University. Currently Prof. Laurent' researches focus on the synthesis of carbon nanotubes and graphene (notably the selectivity on the number of walls/layers), ceramic- and metal-matrix nanocomposites, and spark plasma sintering. He has published more than 110 papers in peer-reviewed journals.

E-mail : [laurent@chimie.ups-tlse.fr](mailto:laurent@chimie.ups-tlse.fr)